



Phase Separation in Ternary Fluid Mixtures: A Molecular Dynamics Study

Journal:	<i>Soft Matter</i>
Manuscript ID:	SM-ART-12-2014-002726.R1
Article Type:	Paper
Date Submitted by the Author:	16-Jan-2015
Complete List of Authors:	Singh, Awaneesh; Jawaharlal Nehru University, School of Physical Sciences Puri, Sanjay; Jawaharlal Nehru University, School of Physical Sciences

Phase Separation in Ternary Fluid Mixtures: A Molecular Dynamics Study

Awaneesh Singh, and Sanjay Puri

School of Physical Sciences, Jawaharlal Nehru University, New Delhi–
110067, India.

Abstract

We present detailed results from molecular dynamics (MD) simulations of phase separation in ternary (ABC) fluid mixtures for $d = 2$ and $d = 3$ systems. Our MD simulations naturally incorporate hydrodynamic effects. The domain growth law is $\ell(t) \sim t^\phi$ with dynamic growth exponent ϕ . Our data clearly indicates that a ternary fluid mixture reaches a dynamical scaling regime at late times with a gradual crossover from $\phi = 1/3 \rightarrow 1/2 \rightarrow 2/3$ in $d = 2$ and $\phi = 1/3 \rightarrow 1$ in $d = 3$ resulting from the hydrodynamic effect in the system. These MD simulations do not yet access the inertial hydrodynamic regime (with $\ell(t) \sim t^{2/3}$) of phase separation in ternary fluid mixtures in $d = 3$.

1 Introduction

A mixture of incompatible fluids, which is homogeneous at high temperature phase separate into domains when quenched below its critical temperature. A good amount of research interests have focused on the kinetics of phase separation of homogeneous multicomponent mixtures due to its scientific and technological importance. After the quench, the final equilibrium state is one in which the pure phases are separated by a single connected interface; however, in the thermodynamic limit, this equilibrium state is never achieved. In view of this, the kinetics of the phase separation process gains importance. Studies in this *far-from-equilibrium* evolution have primarily focused on binary (AB) fluid mixtures where an evolving system segregates into A - and B -rich domains. These domains coarsen with time because it is energetically favorable to eliminate domain interfaces. While phase separation dynamics in AB mixture has been studied extensively theoretically [1, 2, 3] and experimentally [4, 5, 6, 7, 8, 9], the growth dynamics in ternary mixtures are still poorly understood. It is because, in ternary mixture, phase-ordering competition significantly increases the complexity of the problem. However, some experimental techniques have been attempted to control phase-separation dynamics during the macrophase separation process [10, 11].

It is now well-established that the growth of domains during the phase separation is a scaling phenomenon, e.g., the two-point equal-time *correlation function* $C(r, t)$ and its Fourier transform, the *structure factor* $S(k, t)$, characterizing the domain morphology and growth, exhibits the dynamical scaling form [12, 13]:

$$\begin{aligned} C(r, t) &= g[r/\ell(t)], \\ S(k, t) &= \ell(t)^d f[k\ell(t)]. \end{aligned} \tag{1}$$

Here, $g(x)$ and $f(p)$ are the scaling functions; r is the separation between two spatial points; k is the magnitude of the wave vector; and d is the system dimensionality. Dynamical scaling is characterized by the single time-dependent length scale $\ell(t)$. Typically, length scale $\ell(t)$ is considered as the average domain size which follows a simple power-law dependence on time: $\ell(t) \sim t^\phi$, where ϕ represents the exponent characteristic of the universality class to which the system belongs [1, 2, 3].

The coarsening mechanisms can be either diffusive (e.g., binary alloys) or hydrodynamic (e.g., binary fluids), and the growth law depends on the

relevant coarsening mechanism [2]. If growth is driven by diffusion, we have $\ell(t) \sim t^{1/3}$ for dimensionality $d \geq 2$, which is referred to as the Lifshitz-Slyozov (LS) growth law [14]. If the primary growth mechanism is hydrodynamic, ϕ takes a range of different values—depending on the time regime and the dimensionality ($\phi \sim 1/3 \rightarrow 1/2 \rightarrow 2/3$ in $d = 2$ and $\phi \sim 1/3 \rightarrow 1 \rightarrow 2/3$ in $d = 3$) [15]. The diffusive regime has been observed in many experiments and simulations [16, 17, 18]. For $d = 3$, the viscous hydrodynamic regime ($\phi = 1$) has also been observed in many simulations. These include studies of coarse-grained models like *Model H* or its variants [19, 20, 21]. However, it has proven harder to observe the linear growth regime with microscopic-level [molecular dynamics (MD)] simulations where hydrodynamic effects are naturally included. An unambiguous confirmation of this regime has only been provided by MD simulations of Ahmad et al. [22] for simple binary fluids, and more recently by Singh et al. [23] for binary polymeric fluid mixtures.

Finally, the inertial regime in $d = 3$ with $\ell(t) \sim t^{2/3}$ has only been observed numerically in *lattice Boltzmann* simulations [24, 25], which are analogous to coarse-grained phenomenological models. To date, MD simulations have not accessed the inertial growth regime as this is computationally very demanding for $d = 3$ systems [22]. There has also been considerable discussion in the literature about growth exponents for $d = 2$ phase-separating fluid mixtures [26, 27, 28, 29]. The consensus appears to be that there is a crossover from $\phi = 1/3$ (diffusive regime) to $1/2$ (viscous hydrodynamic regime) to $2/3$ (inertial hydrodynamic regime).

To place our work in the proper context, let us briefly review some closely related studies on ternary (*ABC*) fluid mixtures. Laradji et al. (LMT) [30] have undertaken an MD study of segregation kinetics of a symmetric ternary fluid mixture in $d = 2$. LMT found that the hydrodynamic flow does not control the phase-separation process even at “late” stages of the evolution, as it does for the critically quenched binary fluid mixture. Their results suggest that a ternary fluid mixture at late stages follows the growth law $\ell \sim t^{1/3}$, in agreement with the classical theory by Lifshitz and Slyozov. LMT simulation can not genuinely be termed a “late-stage” study as they only access the diffusive or Lifshitz-Slyozov (LS) ($\phi = 1/3$) regime. In a more recent work, Lakshmi et. al. (LK) [31] presented results from hydrodynamic lattice-gas simulations of the binary and ternary fluid mixtures in $d = 2$. In the symmetric ternary mixture with equal surface tension between different interfaces and equal volume fractions, LK observed the diffusive growth regime ($\ell \sim t^{1/3}$) at earlier times. At late times, they observed a crossover to

$\ell \sim t^{1/2}$ growth regime. They have also reported that the growth exponent changes to $2/3$ by reducing the volume fraction of one of the components.

In another class of works, Tafa et. al. (TPK) [32] has undertaken a Monte Carlo (MC) study of phase-separation kinetics in ternary mixtures in $d = 2$. Though the system is purely diffusive, it is worth to mention here. They have considered an asymmetric ternary mixture, where the composition of one of the components (C , termed as vacancy V) is very small. Depending on the possible interactions (between A , B , and C particles) TPK has discussed three distinct evolution morphologies—two phase (AV -rich and BV -rich) coexistence; three-phase coexistence with coating (only AV and BV interfaces); and three-phase coexistence with blobs (all possible interfaces).

Though all the techniques mentioned in the previous paragraph for ternary fluid mixtures that are studied in $d = 2$, our understanding in $d = 3$ systems are rather untouched. In this paper, we undertake a comprehensive MD simulation study of phase-separation kinetics in ternary fluid mixtures in $d = 2$ and $d = 3$. In our MD simulations, we consider both symmetric and asymmetric mixtures with equal interaction between all possible interfaces. Along with this, we will also compare it with the well studied case of phase-separation kinetics in binary fluid mixture. In particular, we will focus on the range of possible morphologies as measured by the correlation function and structure factor of the segregating mixtures depending on the compositions of A , B , and C particles, and the corresponding dynamical behaviors as characterized by various standard tools. Our MD results provide the first unambiguous confirmation of a crossover from the diffusive to the viscous hydrodynamic regime for ternary fluid mixtures in $d = 3$. Also, for $d = 2$ systems, this is the first such observation, as far as MD results are concerned.

This paper is organized as follows. In Sec. 2, we describe the details of the model and simulation methods. We present comprehensive MD results for both structure and dynamics in $d = 2$ and $d = 3$ in Sec. 3. Finally, Sec. 4 concludes this paper with a summary and discussion.

2 Model and Simulation Methods

Let us start with a description of our MD simulation for the study of phase separation in ternary fluids. We consider Lennard-Jones (LJ) particles of diameter σ placed in a continuous space in a box of size $(L_s\sigma)^d$ subject

to periodic boundary conditions. The potential acting between any pair of particles at distance $r_{ij} = |\vec{r}_i - \vec{r}_j|$ is the truncated and shifted Lennard-Jones potential $V(r_{ij})$ with a cut-off radius, $r_c = 2.5\sigma$. It is defined by [33, 34]

$$V(r_{ij}) = \begin{cases} u_{\text{LJ}}(r_{ij}) - u_{\text{LJ}}(r_c) - (r_{ij} - r_c) \left(\frac{du_{\text{LJ}}}{dr_{ij}} \right)_{r_{ij}=r_c}, & r_{ij} \leq r_c; \\ 0, & r_{ij} > r_c, \end{cases} \quad (2)$$

where u_{LJ} is the standard LJ potential:

$$u_{\text{LJ}}(r) = 4\epsilon_{\alpha\beta} \left[\left(\frac{\sigma}{r_{ij}} \right)^{12} - \left(\frac{\sigma}{r_{ij}} \right)^6 \right]. \quad (3)$$

In Eq. (3), $\epsilon_{\alpha\beta}$ is the interaction strength between α and β [$\in (A, B, C)$] particles. The subtraction of $u_{\text{LJ}}(r_c)$ and a linear term $\propto (r_{ij} - r_c)$ from the LJ potential in the right hand side of Eq. (2), ensures that both the potential and the forces are continuous for all values of r_{ij} . This is required when one considers a dynamic behavior as force discontinuity results in a drift of the total energy in a microcanonical simulation.

The LJ energy parameters are chosen as

$$\begin{aligned} \epsilon_{AA} &= \epsilon_{BB} = \epsilon_{CC} = \epsilon, \\ \epsilon_{AB} &= \epsilon_{BC} = \epsilon_{CA} = \epsilon/2, \end{aligned} \quad (4)$$

so that phase separation is favored energetically. All particles are assigned equal masses:

$$m_A = m_B = m_C = m, \quad (5)$$

and the reduced temperature T^* is chosen as

$$T^* = k_B T / \epsilon. \quad (6)$$

We set m , σ , ϵ , and k_B to unity. We consider the total number of particles $N = N_A + N_B + N_C$ confined in a box of size $(L_s\sigma)^d$ such that the reduced density

$$\rho^* = \rho\sigma^d = N\sigma^d / (L_s\sigma)^d. \quad (7)$$

We used high-density continuum model of LJ particles with $\rho^* = 1$ in $d = 3$; and $\rho^* = 0.8$ in $d = 2$. For these parameters, the LJ system is then in its

liquid phase in the temperature regime of interest. In our simulations, we quench the system at $T = 0.5$ for $d = 2$; and at $T = 1.0$ for $d = 3$. As we show subsequently, this quench temperature is well below the corresponding critical temperature for phase separation. We use the standard *velocity Verlet* algorithm to perform the MD runs. The integration time step is set to $\Delta t = 0.001t_0$, with the LJ time unit

$$t_0 = (m\sigma^2/\epsilon)^{1/2} = 1, \quad (8)$$

which provides integration errors within acceptable limits [33, 34].

The *Nosé-Hoover thermostat* (NHT) [35, 36, 37] is used to control the temperature T . This is known to preserve the hydrodynamics [38, 39] well, and is relatively simple to implement. Of course, more advanced thermostats have recently become available with better hydrodynamics-preserving capability [40, 41]. However, the NHT is adequate for our simulation. Here, the system Hamiltonian is extended by a variable, representing the thermostat, which has a fictitious mass Q [35, 36]. Newton's equations of motion are then generalized to include a *friction* term:

$$\frac{d\vec{v}_i}{dt} = \frac{d^2\vec{r}_i}{dt^2} = \vec{f}_i - \gamma(t)\vec{v}_i, \quad (9)$$

where \vec{f}_i is the *force* term. The friction coefficient $\gamma(t)$ fluctuates in time around zero, obeying the equation

$$\frac{d\gamma}{dt} = \frac{1}{Q} \left(\sum_{i=1}^N \vec{v}_i^2 - 3NT \right). \quad (10)$$

The magnitude of Q determines the coupling between the reservoir and the system and thereby influences the temperature fluctuations. A very large value of Q (loose coupling) may cause a poor temperature control: NHT with $Q \rightarrow \infty$ ($|\gamma(t)| = 0$) generates a microcanonical ensemble [36]. On the other hand, too small values of Q (tight coupling) may cause high-frequency temperature oscillations; in that case the temperature control will not be efficient. We find that $Q = 80$ is sufficient to generate a canonical ensemble in our simulation.

3 Numerical Results

3.1 Characterization of morphologies

In this section, we present results for both structure and dynamics of phase-separating ternary fluid mixtures. The evolution morphologies are characterized by the two-point ($\vec{r} = \vec{r}_1 - \vec{r}_2$) equal-time correlation function and its Fourier transform, the structure factor. Here, we have two kinds of correlation functions. The first one is defined as follows:

$$C(\vec{r}, t) = \langle \psi(\vec{r}_1, t) \psi(\vec{r}_2, t) \rangle - \langle \psi(\vec{r}_1, t) \rangle \langle \psi(\vec{r}_2, t) \rangle, \quad (11)$$

where $\psi(\vec{r}_1, t)$ is the order parameter at a discrete site \vec{r}_1 at time t . The angular brackets indicate an ensemble average. This correlation function refers to the domain morphology of A - and B -particles. The second correlation function of $\psi(\vec{r}_1, t)^2$ is also defined in a similar fashion as follows [32]:

$$D(\vec{r}, t) = \langle \psi(\vec{r}_1, t)^2 \psi(\vec{r}_2, t)^2 \rangle - \langle \psi(\vec{r}_1, t)^2 \rangle \langle \psi(\vec{r}_2, t)^2 \rangle, \quad (12)$$

and refers to the domain morphology of C -particles. We also studied the structure factor, which is the Fourier transform of $C(\vec{r}, t)$:

$$S_c(\vec{k}, t) = \int d\vec{r} e^{i\vec{k}\cdot\vec{r}} C(\vec{r}, t), \quad (13)$$

where \vec{k} is the scattering wave-vector. Similarly, the Fourier transform of $D(\vec{r}, t)$ is denoted by $S_D(\vec{k}, t)$. Since the system is isotropic, we can improve statistics by spherically averaging the correlation function and the structure factor. The corresponding quantities are denoted as $C(r, t)$, $S_c(k, t)$, $D(r, t)$, and $S_D(k, t)$, respectively.

The fundamental assumption of scaling states that there exists a single length scale $\ell(t)$. This results in a scaling behavior shown in Eq. (1). The characteristic domain size $\ell(t)$ is obtained as the distance over which the correlation function decays to some fraction of its maximum value [$C(r, t)=1$, and $D(r, t)=1$ at $r = 0$]. We find that the first zero of $C(r, t)$ and $D(r, t)$ give a good measure of the average domain size $\ell_C(t)$ and $\ell_D(t)$, respectively. There are several other suitable definitions for computing $\ell(t)$, e.g., half-crossing of the correlation function, inverse of the first moment of the structure factor. In the scaling regime, all these definitions differ only by constant multiplicative factors [16].

3.2 Ternary Mixtures in $d = 2$

In this section, we re-examine the previously studied case of ternary fluid coarsening following a critical quench by LMT [30]. Our simulations are carried out for a total number of $N = 52428$ particles of type A , B , and C , randomly distribute in a box of size $(L_s\sigma)^2 = (256\sigma)^2$ such that the density $\rho^* = 0.8$. The periodic boundary conditions are applied in all directions and the results are obtained by averaging over ten independent runs. The homogeneous initial configuration is prepared at a high temperature $T = 10$ for 5×10^5 MD steps. At time $t = 0$, we quench the system from the high-temperature homogeneous phase to a temperature $T = 0.5$ and then monitored the evolution of the system at various times.

In Fig. 1, we present evolution snapshots of the ternary fluid mixtures obtained from our MD simulations at $t = 3000, 12000$. Figures 1(a)-(b) show the evolution pictures for symmetric (1:1:1) and asymmetric (2:2:1) mixtures, respectively. Immediately after the quench, one sees a clear evolution of three kinds of domains, namely, A , B , and C rich with all three kinds of interfaces (AB , BC , and CA) present. In the evolution pictures, A 's are marked in blue; B 's are marked in red and C 's are marked in yellow. In Fig. 1(a), all particles are in equal proportions, we term this as the ‘‘blob’’ morphology [32]. In Fig. 1(b), we show the evolution with reduced C -particles (with corresponding increase in A - and B - particles) and observe the beginning of formation of bicontinuous domain structures between A - and B -rich domains. Figure 1(c) shows the evolution snapshots of a binary fluid mixture (1:1:0) at different times. As expected for a symmetric (critical) composition, a bicontinuous domain structure is seen.

Figure 2 shows a comparison of the scaling functions for the evolutions shown in Fig. 1 at $t = 12000$. For analysis of the results, the order parameter $\psi(\vec{r}, t)$ is obtained by considering non-overlapping boxes of size $(2\sigma)^2$. The continuum fluid configurations are now mapped onto a square lattice of size $(128\sigma)^2$. We count the number of A , B , and C particles in each box. A box effectively occupied by an A particle is assigned the order parameter $\psi(\vec{r}, t) = +1$, that occupied by a B particle is assigned $\psi(\vec{r}, t) = -1$, and that occupied by a C particle is assigned $\psi(\vec{r}, t) = 0$ *i.e.*, $\psi(\vec{r}, t) \in (\pm 1, 0)$. For boxes with equal number of particles, we assign $\psi = +1$ or $\psi = -1$ or $\psi = 0$ with equal probability. Similarly, for binary mixture, we assign $\psi(\vec{r}, t) = +1$ and -1 for A and B particles, respectively [23, 32]. In Fig. 2(a), we plot data for $C(r, t)$ vs. r/ℓ_C , where ℓ_C is defined as the first zero of $C(r, t)$.

The symbols refer to the scaled correlation function for ternary mixtures and the solid line refers to the binary mixture (also computed numerically). The reasonable data collapse demonstrates that the evolving systems belong to the same dynamical universality class. It is also evident from the fact that the order parameter $\psi(\vec{r}, t) = 0$ does not contribute in the calculation of the correlation function. Therefore, the scaling behavior of $C(r, t)$ for a ternary mixture should be comparable to that of a binary mixture. In Fig. 2(b), we show the scaled $D(r, t)$ at $t = 12000$ for two compositions of ternary mixtures as denoted by the indicated symbols. Here, the definition of $D(r, t)$ is equivalent to that for a binary mixture with off-critical composition and it is well known that the correlation function varies continuously with the degree of off-criticality [1, 42]. For a binary mixture $D(r, t) = 0 \forall r$. The scaled correlation function clearly depends upon the compositions of A , B and C particles.

Next, we focus on the time dependence of the domain size. In Fig. 3, we show a plot of $\ell_C(t)$ vs. t on a log-log scale for the evolution shown in Fig. 1. The dashed lines show the expected growth exponents in various growth regimes for $d = 2$ fluids. Our data for binary mixture (solid line) clearly shows all growth regimes as discussed earlier. After an early transient regime, the data sets for ternary mixtures (represented by corresponding open symbols) follow the diffusive growth law (or Lifshitz-Slyozov growth): $\ell_C(t) \sim t^{1/3}$. This growth regime appears to be very short-lived and a gradual crossover to a viscous hydrodynamic regime ($\phi = 1/2$) appears as early as $t \gtrsim 600$, extending over a large fraction of the time window. Our results contradict the finding of LMT [30], the only MD simulation till date for the phase separation kinetics in a symmetric (1:1:1) ternary mixture. The possible reason that LMT could not see the crossover from $t^{1/3} \rightarrow t^{1/2}$ is that their simulation access only the diffusive regime. In such a case, due to a lack of connectivity between domains, it might reasonably eliminate the hydrodynamic transport. At late times ($t > 5000$), our data clearly approaching $\phi = 2/3$ exponent, an inertial hydrodynamic regime on the time-scale of our simulation. However, as C -particle composition is increased, evolution time-scale become slower.

3.3 Ternary Mixtures in $d = 3$

We consider a total number of $N = 110592$ particles confined in a cubic box of size $(L_s\sigma)^3 = (48\sigma)^3$ such that $\rho^* = 1$ with periodic boundary conditions in all directions. The homogeneous initial configurations are prepared by

equilibrating the system at $T = 10$. At $t = 0$, the system is quenched at $T = 1$.

Figure 4(a)-(c) show typical evolution morphologies from a homogenous initial condition. We show the evolution pictures at $t = 1000$, and 5000. Figure 4(a) corresponds to a quench for a symmetric (1:1:1) ternary mixture. One can see a clear evolution of A , B , and C rich domains (termed as a “blob” morphology). The evolution in Fig. 4(b) corresponds to an asymmetric (2:2:1) ternary mixture. Here, we observe few imprints of bicontinuous domains between A - and B -rich phases. Figure 4(c) shows the evolution of a binary mixture (1:1:0) with critical composition.

Next, we focus on the various statistical properties of the evolution depicted in Fig. 4. First, we discuss the blob morphology then compare with other morphologies, mainly highlighting differences from the blob morphology. In $d = 3$ simulation, the order parameter $\psi(\vec{r}, t)$ is obtained by following the same approach as for $d = 2$ system. Here, we consider the non-overlapping boxes of size $(1.5\sigma)^3$. The system is now mapped onto a simple cubic lattice of size $(32\sigma)^3$. All the results presented here are obtained by averaging over ten independent runs. In Fig. 5, we show the dynamical scaling of $C(r, t)$ and $D(r, t)$ for the evolution shown in Fig. 4(a). Figure 5(a) superposes data for $C(r, t)$ as a function of the scaled distance r/ℓ_C at three times, as indicated. The data from different times collapses onto a single master curve reasonably well, showing that the scaling regime has been reached. Figure 5(b) is the corresponding scaling plot of $D(r, t)$ vs. r/ℓ_D . The good data collapse in Fig. 5(b) also confirms the dynamical scaling. Figure 5 shows that $C(r, t)$ and $D(r, t)$ do not differ appreciably from each-other due to the equal composition of A , B , and C particles. More substantial differences are seen when particles are present in different proportions. The correlation function data for the morphologies shown in Figs. 4(b) and 4(c) also exhibit a dynamical scaling. For brevity, we do not present this data here.

We now discuss whether the evolution morphology depends on the composition ratios of the particles. Figure 6 shows a comparison of the scaled correlation functions and the corresponding structure factors for three different compositions at $t = 5000$, when the system is already in the scaling regime. In Fig. 6(a), we plot $C(r, t)$ vs. r/ℓ_C for ternary mixtures, denoted by the indicated symbols. For a reference, the scaled correlation function for a binary mixture, denoted by a solid line is also included. We observe that the data sets (for ψ -field) collapse nicely onto a master function and therefore, suggest that they belong to the same dynamical universality class.

A log-log plot of $S_c(k, t)\ell_C^{-3}$ vs. $k\ell_C$ is shown in Fig. 6(b), also demonstrating dynamical scaling. For large values of k , $S_c(k, t)$ follows the well-known Porod's law, $S_c(k, t) \sim k^{(d+1)}$, which results from scattering off sharp interfaces [43, 44]. In Fig. 6(c), we present the scaling behavior of $D(r, t)$ vs. r/ℓ_D and Figure 6(d) shows the corresponding time-dependent behavior of structure factor: $S_D(k, t)\ell_D^{-3}$ vs. $k\ell_D$. The scaling functions clearly depend upon the composition ratios of A , B and C particles.

In Fig. 7, we turn our attention to the time-dependence of domain size for the evolution shown in Figs. 4. In Fig. 7, we plot $\ell_C(t)$ vs. t on a log-log scale for ternary mixtures as indicated by open symbols. For reference, we also plot $\ell_C(t)$ vs. t for a binary mixture, indicated by a solid line. After an initial transient, the growth law is consistent with the diffusive regime, i.e., $\ell_C(t) \sim t^{1/3}$. At later times, hydrodynamic effects become important and domain growth gradually evolves towards the viscous hydrodynamic regime ($\phi = 1$). For the symmetric (1:1:1) mixture, the evolution time-scale appears a bit slow due to lack of connectivity between domains which might affect the hydrodynamic transport. For the asymmetric mixtures (A and B particles are increased at the cost of C), the connectivity between A and B domains are increased; now, the hydrodynamic transport becomes more effective and so the evolution time-scale becomes faster.

Our simulation data sets clearly show a gradual crossover from $t^{1/3} \rightarrow t^1$ for ternary mixtures, but we have not accessed the $t^{2/3}$ -regime on the time-scale of our simulation. This is not surprising as the inertial regime has not even been observed in MD simulations of binary fluids. Ahmad et al. [22] have estimated that significantly larger numerical effort is required to access the $t^{2/3}$ -growth regime in phase-separating simple binary fluids. However, our simulation results strongly support the contention that the hydrodynamic flow should control the phase-separation process in ternary fluids at late stages.

4 Summary and Discussion

Let us conclude this paper with a summary and discussion of our results. We present results from a *molecular dynamics* (MD) simulation for the evolution of phase-separating ternary immiscible mixtures. The simulations are carried out in $d = 2$ and $d = 3$ systems. The *Lennard-Jones* (LJ) potential (truncated and shifted) is applied between any pair of particles. Our MD

approach has an advantage that it naturally incorporates the hydrodynamic effects. The *Nosé-Hoover thermostat* (NHT) is used to generate a canonical ensemble and is well-known to preserve hydrodynamic effects.

We discuss the various morphologies of phase-separating ternary fluid mixtures by changing the compositions of particles. The scaling forms of $C(r, t)$ and $S_c(k, t)$ appear to be independent of the particle composition for $d = 2$ as well as $d = 3$ systems. However, $D(r, t)$ and $S_D(k, t)$ clearly depend on the particle compositions. It is found that the early-time domain growth law is always consistent with the Lifshitz-Slyozov (LS) growth law. Our results clearly suggest that it is the hydrodynamic flow which dominates the late-time dynamics of ternary mixtures. In $d = 2$, we observe a crossover from $\ell_C \sim t^{1/3} \rightarrow t^{1/2} \rightarrow t^{2/3}$. In $d = 3$, we observe a crossover from a diffusive regime to a viscous hydrodynamic regime ($\ell_C \sim t^{1/3} \rightarrow t^1$). This is the first such significant observation in ternary fluid mixtures. For $d = 3$ fluids, we also expect an asymptotic inertial regime with $\ell_C \sim t^{2/3}$. However, this requires considerably larger computational effort [22]. We hope the present study will stimulate further MD simulations and experiments on this problem.

Acknowledgments

SP and AS acknowledge the J. C. Bose fellowship of the Department of Science and Technology, India, for providing financial support.

References

- [1] S. Puri, and V. K. Wadhawan, (Editors), *Kinetics of Phase Transitions* (CRC Press, Boca Raton, Fla.) 2009.
- [2] A. J. Bray, *Adv. Phys.*, 1994, **43**, 357.
- [3] A. Onuki, *Phase Transition Dynamics* (Cambridge University Press, Cambridge) 2002.
- [4] J. Lal, and R. Bansil, *Macromolecules* **24**, 290 (1991).
- [5] H. Tanaka, *Phys. Rev. Lett.* **71**, 3158 (1993).
- [6] H. Tanaka, *Phys. Rev. Lett.* **72**, 2581 (1994).
- [7] H. Tanaka, *J. Chem. Phys.* **100**, 5323 (1994).
- [8] C. K. Haas, and J. M. Torkelson, *Phys. Rev. E* **55**, 3191 (1997).
- [9] P. Xavier, A. Bharati, G. Madras, and S. Bose, *Phys. Chem. Chem. Phys.*, **16**, 21300 (2014).
- [10] Q. Tran-Cong-Miyata, S. Nishigami, T. Ito, S. Komatsu, and T. Norisuye, *Nat. Mater.*, **3**, 448 (2004).
- [11] L. Yan, and A. C. Balazs, *J. Mater. Chem.*, 21, 14278 (2011).
- [12] K. Binder, and D. Stauffer, *Phys. Rev. Lett.*, 1974, **33**, 1006.
- [13] K. Binder, *Phys. Rev. B*, 1977, **15**, 4425.
- [14] I. M. Lifshitz, and V. V. Slyozov, *J. Phys. Chem. Solids*, 1961, **19**, 35.
- [15] E. D. Siggia, *Phys. Rev. A*, 1979, **20**, 595.
- [16] Y. Oono, and S. Puri, *Phys. Rev. Lett.*, 1987, **58**, 836.
- [17] Y. Oono, and S. Puri, *Phys. Rev. A*, 1988, **38**, 434.
- [18] S. Puri, and Y. Oono, *Phys. Rev. A*, 1988, **38**, 1542.
- [19] T. Koga, and K. Kawasaki, *Phys. Rev. A*, 1991, **44**, R817.

- [20] S. Puri, and B. Dunweg, Phys. Rev. A, 1992, **45**, R6977.
- [21] A. Shinozaki, and Y. Oono, Phys. Rev. E, 1993, **48**, 2622.
- [22] S. Ahmad, S. K. Das, and S. Puri, Phys. Rev. E, 2010, **82**, 040107 (R); 2012, **85**, 031140.
- [23] A. Singh, S. Puri, and C. Dasgupta, J. Chem. Phys., 2014, **140**, 244906.
- [24] V. M. Kendon, J. C. Desplat, P. Bladon, and M. E. Cates, Phys. Rev. Lett., 1999, **83**, 576.
- [25] V. M. Kendon, M. E. Cates, I. Pagonabarraga, J. C. Desplat, and P. Blandon, J. Fluid Mech., 2001, **440**, 147.
- [26] H. Furukawa, Adv. Phys., 1985, **34**, 703.
- [27] F. J. Alexander, S. Chen, and D. W. Grunau, Phys. Rev. B, 1993, **48**, 634.
- [28] E. Velasco, and S. Toxvaerd, Phys. Rev. Lett., 1993, **71**, 388.
- [29] G. Leptoukh, B. Strickland, and C. Roland, Phys. Rev. Lett., 1995, **74**, 3636.
- [30] M. Laradji, O. G. Mouritsen, and S. Toxvaerd, Europhys. Lett., 1994, **28**, 157.
- [31] K. C. Lakshmi, and P. B. SunilKumar, Phys. Rev. E, 2003, **67**, 011507.
- [32] K. Tafa, S. Puri, and D. Kumar, Phys. Rev. E, 2001, **64**, 056139.
- [33] M. P. Allen, and D. J. Tildesley, *Computer Simulation of Liquids* (Clarendon Press, Oxford) 1991.
- [34] D. Frenkel, and B. Smit, *Understanding Molecular Simulation – From Algorithms to Applications* (Academic Press, London) 2002.
- [35] S. Nose, J. Chem. Phys., 1984, **81**, 511; Mol. Phys., 1984, **52**, 255.
- [36] W. G. Hoover, Phys. Rev. A, 1985, **31**, 1695.
- [37] W. G. Hoover, *Time Reversibility: Computer Simulation and Chaos* (World Scientific, Singapore) 1999.

- [38] K. Binder, and G. Ciccotti (Editors), *Monte Carlo and Molecular Dynamics of Condensed Matter Systems* (Italian Physical Society, Bologna) 1996.
- [39] K. Binder, J. Horbach, W. Kob, W. Paul, and F. Varnik, *J. Phys.: Condens. Matter*, 2004, **16**, S429.
- [40] S. D. Stoyanov, and R. D. Groot, *J. Chem. Phys.*, 2005, **122**, 114112.
- [41] M. P. Allen, and F. Schmid, *Mol. Simul.*, 2007, **33**, 21.
- [42] T. M. Rogers, K. R. Elder, and R. C. Desai, *Phys. Rev. B*, 1987, **37**, 9638.
- [43] G. Porod, in *Small-Angle X-Ray Scattering*, O. Glatter and O. Kratky (Editors), (Academic Press, New York) 1982.
- [44] Y. Oono, and S. Puri, *Mod. Phys. Lett. B*, 1988, **2**, 861.

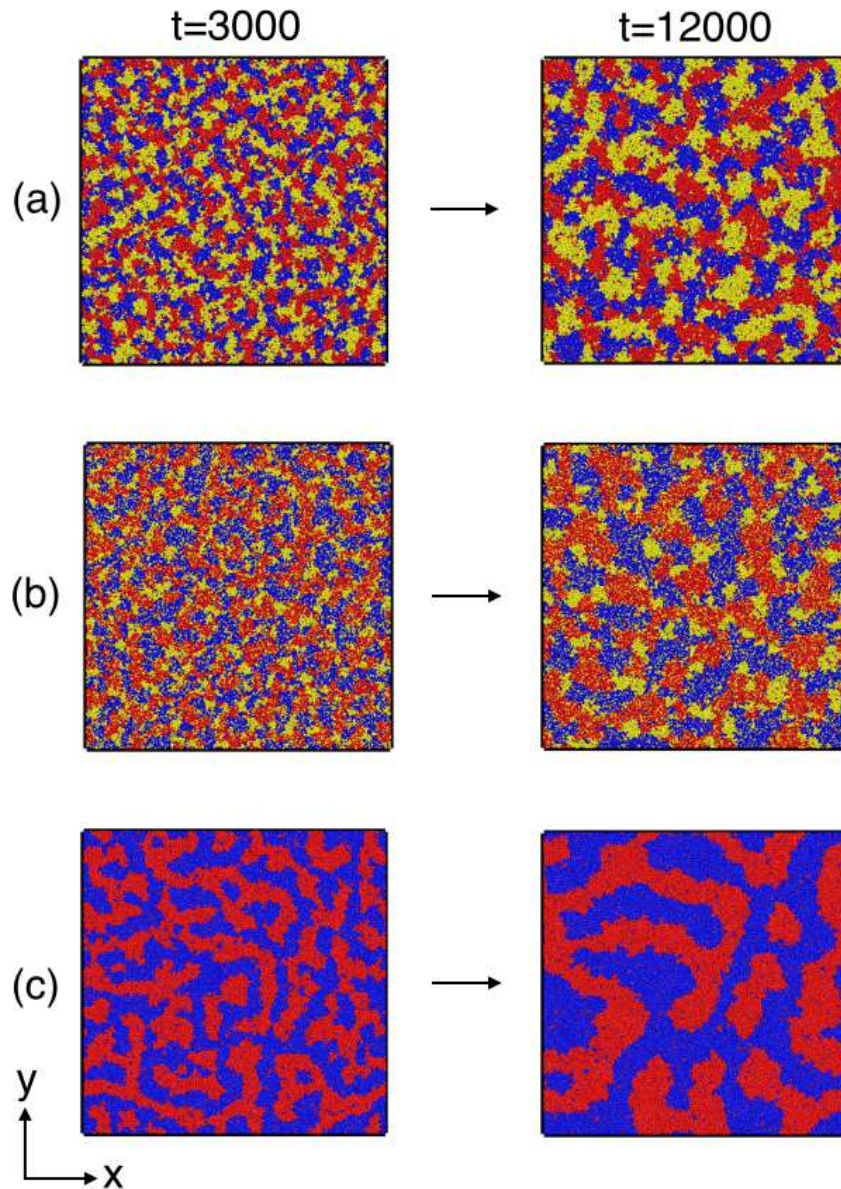


Figure 1: The evolution snapshots for ternary mixtures in $d = 2$ for (a) $A:B:C=1:1:1$, and (b) $A:B:C=2:2:1$, and (c) $A:B:C=1:1:0$ at $t = 3000$, 12000 . The snapshots are obtained from the molecular dynamics (MD) simulations described in the text. Regions with A -atoms are marked blue, B -atoms are marked red and C -atoms are marked yellow.

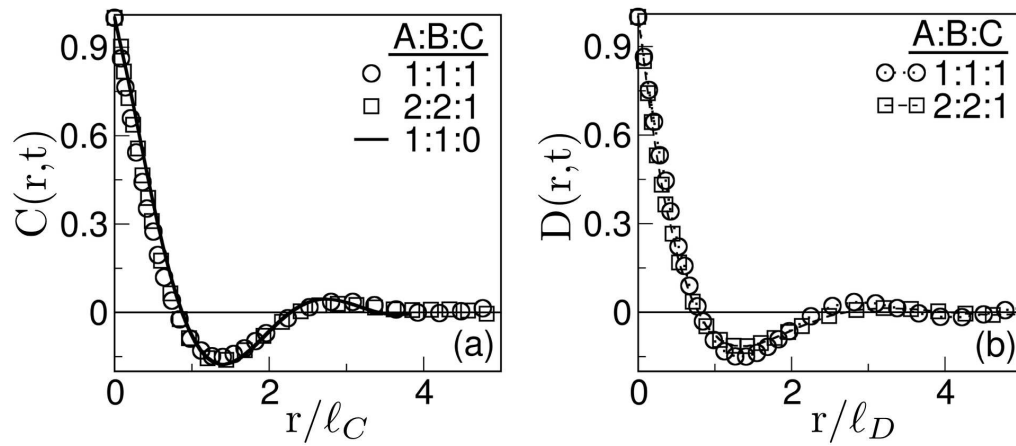


Figure 2: (a) Superposition of numerical data for $C(r,t)$ vs. r/l_C for the evolution shown in Fig. 1 at $t = 12000$ —denoted by the specified symbol type. The solid line refers to the data for binary mixture ($A:B:C=1:1:0$). The correlation function data is obtained as an average over ten independent runs. (b) Superposition of data for $D(r,t)$ vs. r/l_D , corresponding to the data sets of ternary mixtures in (a).

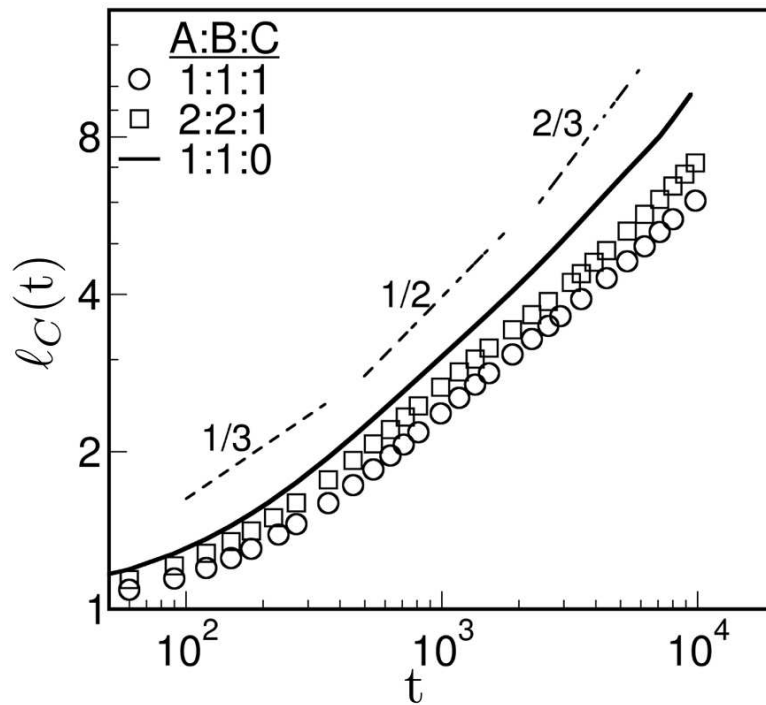


Figure 3: Plot of the characteristic length scale $\ell_C(t)$ vs. t on a log-log scale for the evolutions shown in Fig. 1. The Solid line represents simulation data for binary mixture whereas open symbols represent corresponding ternary mixture data. for The dashed lines of slope $1/3$, $1/2$ and $2/3$ correspond to expected growth regimes for $d = 2$ fluids.

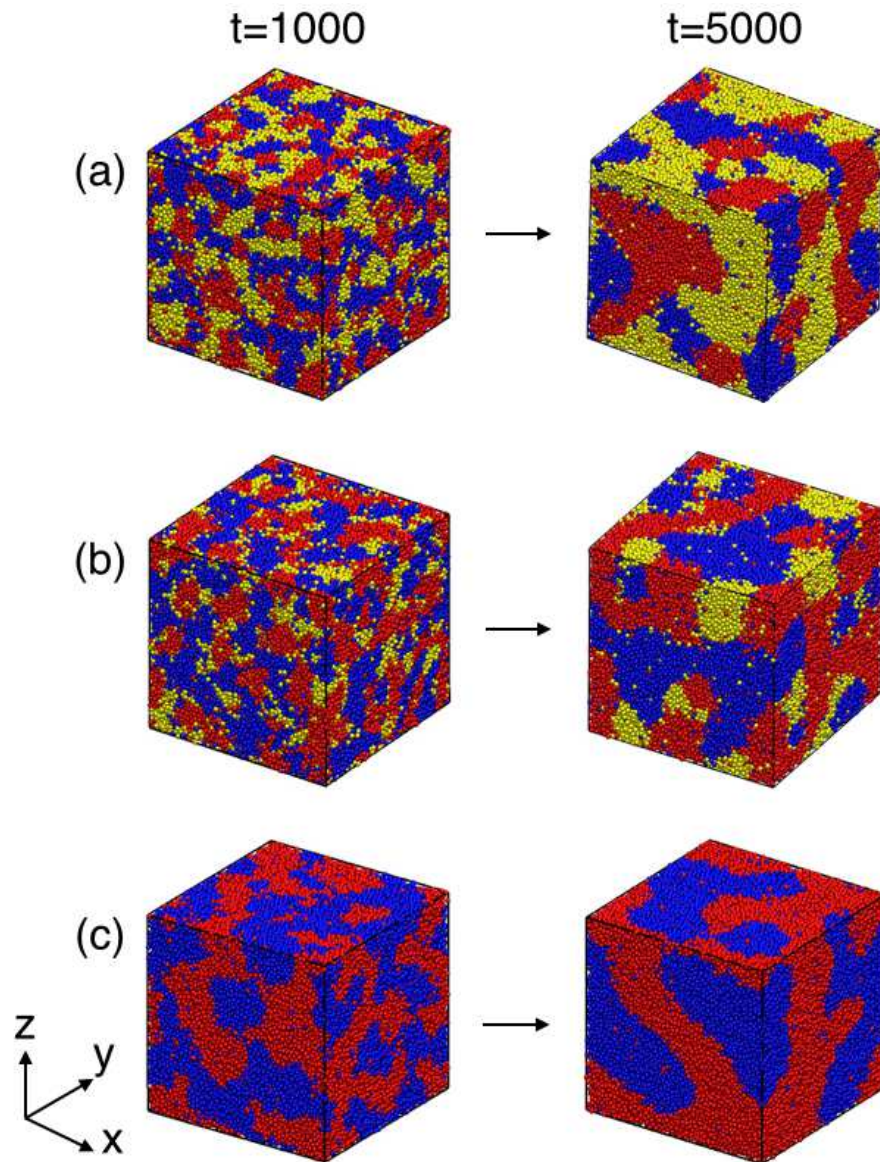


Figure 4: Evolution pictures of phase-separation in ternary mixtures in $d = 3$ for (a) $A:B:C=1:1:1$, and (b) $A:B:C=2:2:1$, and (c) $A:B:C=1:1:0$. The snapshots are taken at $t = 1000$ and 5000 , respectively. The numerical details of our simulations are described in the text.

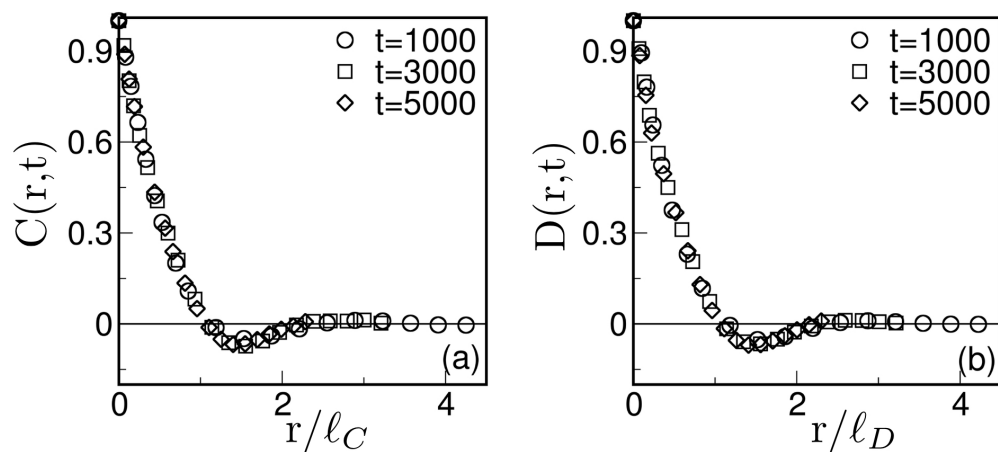


Figure 5: (a) Scaling plot of $C(r,t)$ vs. r/l_C for $A:B:C=1:1:1$. The data sets (for $t = 1000, 3000, 5000$) collapse onto a single master curve. (b) Scaling plot of $D(r,t)$ vs. r/l_D for the same times as in (a).

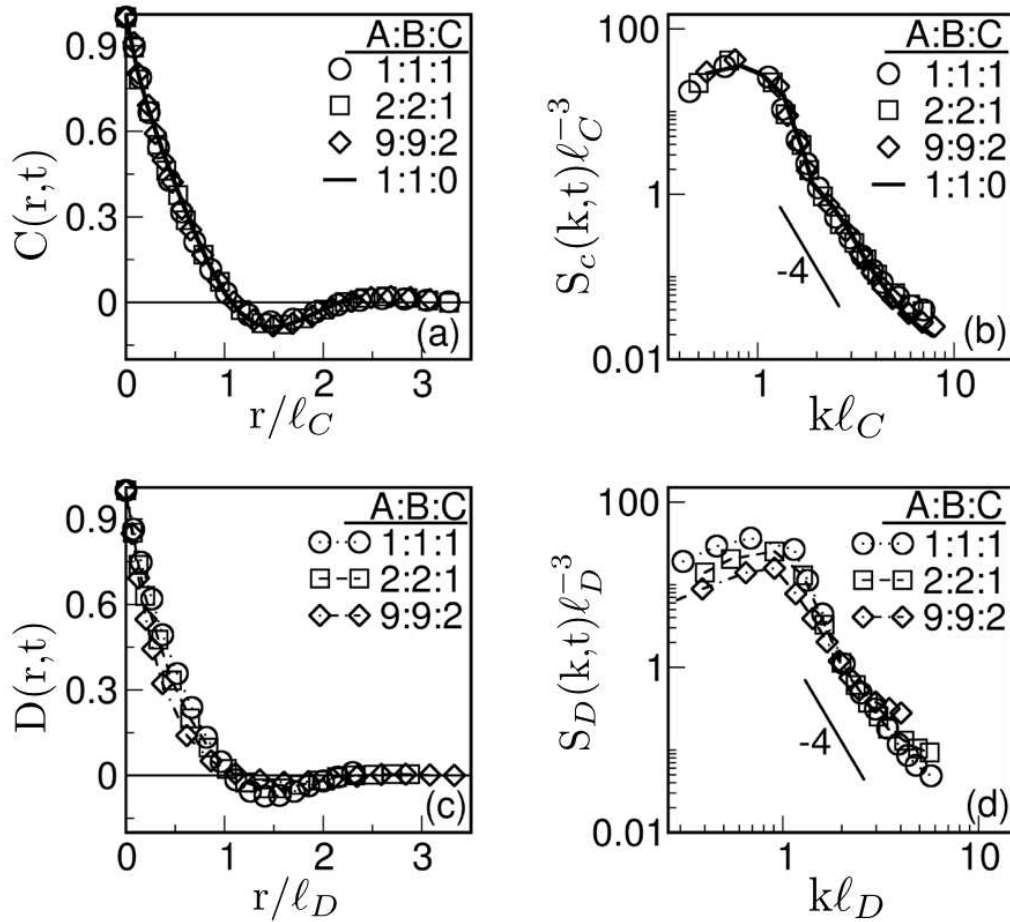


Figure 6: (a) Comparison of $C(r,t)$ vs. r/l_C at $t = 5000$ for the evolutions shown in Fig. 4 (indicated by the symbols). The solid line shows the scaled correlation function for binary mixture. (b) Shows the plot of $S_c(k,t)l_C^{-3}$ vs. kl_C for the same data sets as in (a). The large- k region (tail) of the structure factor obeys the Porod law, $S(k,t) \sim k^{-4}$ for $k \rightarrow \infty$. (c) Superposition of data for $D(r,t)$ vs. r/l_D , and (d) $S_D(k,t)l_D^{-3}$ vs. kl_D for the morphologies in Fig. 4 at $t = 5000$.

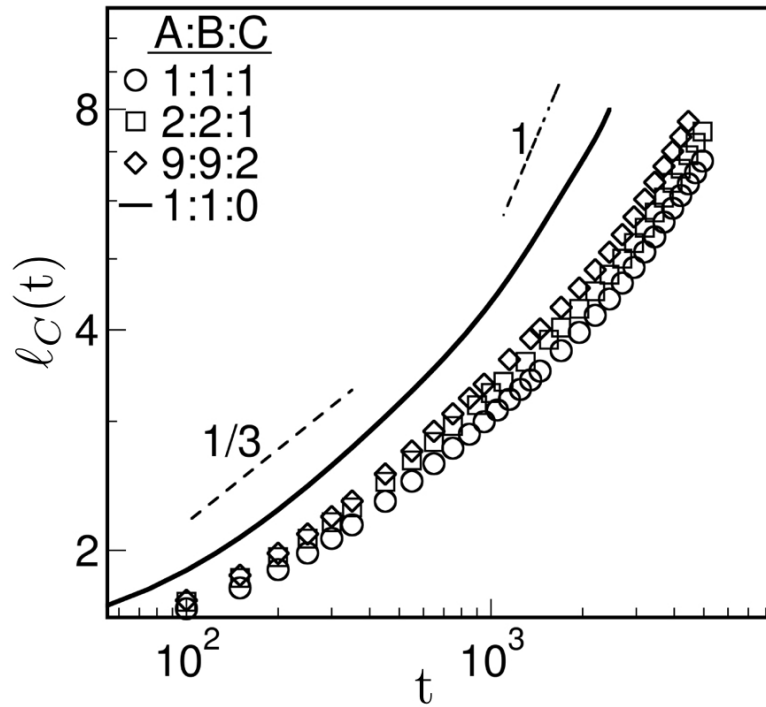
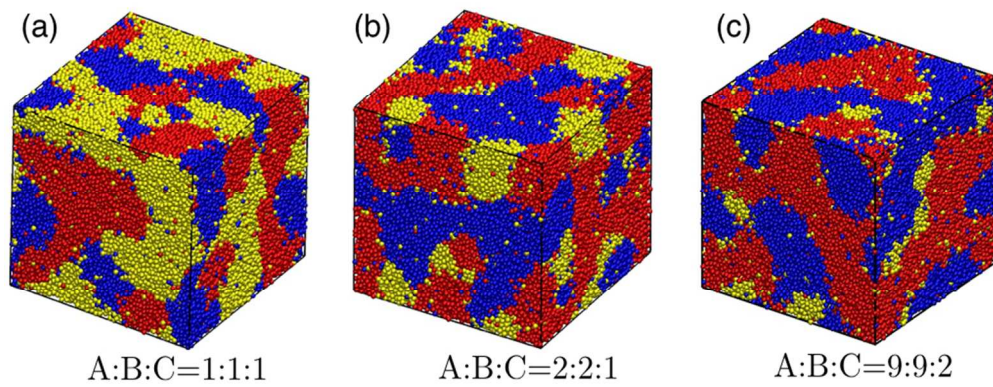


Figure 7: (a) Log-log plot of the time-dependence of the characteristic length scale $\ell_C(t)$ for the evolutions shown in Fig. 4. Solid line and open symbols represent the data sets for binary mixture and ternary mixtures respectively. The error bars on the data points are smaller than the symbol sizes. The lines of slope $1/3$ and 1 correspond to expected growth regimes for $d = 3$ fluids.



Our molecular dynamics simulation results strongly support the contention that the hydrodynamic flow should control the phase-separation process in ternary fluid (ABC) mixtures at late stages.
361x141mm (72 x 72 DPI)

Our molecular dynamics simulation results strongly support the contention that the hydrodynamic flow should control the phase-separation process in ternary fluid (ABC) mixtures at late stages.